QUICK USER GUIDE

DAGMARA OSZKIEWICZ

Contents

1. Introduction

2. Overview of phase functions

Absolute magnitude computation relies on magnitude phase-curve fitting. A number of different mathematical formulations for magnitude phase curves have been developed. Here we make use of the H,G phase function, the H,G_1,G_2 phase function, and the H,G_{12} phase function.

Date: February 17, 2011.

The H,G phase function was developed to predict the magnitude of an asteroid as a function of solar phase angle [Bowell et al. (1989)]. This function was adopted by the International Astronomical Union in 1985 to redefine the absolute magnitudes of asteroids. The H,G phase function is not valid for phase angles greater than 120°.

The H,G_1,G_2 and H,G_{12} phase functions [K. Muinonen et al. (2010)] are based on cubic splines. The H,G_1,G_2 phase function is designed to fit asteroid phase curves containing substantial numbers of observations, whereas the H,G_{12} phase function is applicable to asteroids that have sparse or low-accurancy photometric data.

2.1. H,G **phase function.** In the H,G magnitude phase function, the reduced apparent magnitudes can be obtained from:

$$\begin{aligned} 10^{-0.4V(\alpha)} &= a_1\Phi_1(\alpha) + a_2\Phi_2(\alpha) \\ &= 10^{-0.4H}\left[(1-G)\Phi_1(\alpha) + G\Phi_2(\alpha)\right], \end{aligned} \tag{1}$$

where α is the phase angle, $V(\alpha)$ is the reduced magnitude. The basis functions Φ_1, Φ_2 are defined as:

$$\begin{aligned} \Phi_1(\alpha) &= w\left(1 - \frac{0.986\sin\alpha}{0.119 + 1.341\sin\alpha - 0.754\sin^2\alpha}\right) \\ &+ (1-w)\left(\exp(-3.332\tan^{0.631}\frac{1}{2}\alpha)\right), \\ \Phi_2(\alpha) &= w\left(1 - \frac{0.238\sin\alpha}{0.119 + 1.341\sin\alpha - 0.754\sin^2\alpha}\right) \\ &+ (1-w)\exp\left(-1.862\tan^{1.218}\frac{1}{2}\alpha\right), \\ w &= \exp\left(-90.56\tan^2\frac{1}{2}\alpha\right). \end{aligned} \tag{2}$$

The coefficients a_1 and a_2 are estimated from observations using linear least squares. The absolute magnitude H and slope parameter G, can then be obtained from:

$$H = -2.5\log_{10}(a_1 + a_2), \tag{3}$$

$$G = \frac{a_2}{a_1 + a_2}. \tag{4}$$

2.2. H,G_1,G_2 **phase function.** The reduced magnitudes $V(\alpha)$ can be obtained from [K. Muinonen et al. (2010)]:

$$\begin{aligned} 10^{-0.4V(\alpha)} &= a_1\Phi_1(\alpha) + a_2\Phi_2(\alpha) + a_3\Phi_3(\alpha) \\ &= 10^{-0.4H}\left[G_1\Phi_1(\alpha) + G_2\Phi_2(\alpha) + (1 - G_1 - G_2)\Phi_3(\alpha)\right], \end{aligned}$$

(5)

where the absolute magnitude H and slope parameters G_1, and G_2 are:

$$H = -2.5\log_{10}(a_1 + a_2 + a_3), \tag{6}$$

$$G_1 = \frac{a_1}{a_1 + a_2 + a_3}, \tag{7}$$

$$G_2 = \frac{a_2}{a_1 + a_2 + a_3}. \tag{8}$$

The coefficients a_1, a_2, a_3 are estimated from the observations using linear least squares. The basis functions $\Phi_1(\alpha)$, $\Phi_2(\alpha)$, $\Phi_3(\alpha)$ are defined as:

- For $0° < \alpha \leq 7.5°$:
  - $\Phi_1(\alpha) = 1 - \frac{6}{\pi}\alpha$;
  - $\Phi_2(\alpha) = 1 - \frac{9}{5\pi}\alpha$;
  - $\Phi_3(\alpha)$ is defined using a cubic spline as defined in Table 2.
- For $7.5° < \alpha \leq 30°$:
  - $\Phi_1(\alpha)$ is defined using a cubic spline as defined in Table 1;
  - $\Phi_2(\alpha)$ is defined using a cubic spline as defined in Table 1;
  - $\Phi_3(\alpha)$ is defined using a cubic spline as defined in Table 2.
- For $30° < \alpha \leq 150°$:
  - $\Phi_1(\alpha)$ is defined using a cubic spline as defined in Table 1;
  - $\Phi_2(\alpha)$ is defined using a cubic spline as defined in Table 1;
  - $\Phi_3(\alpha) = 0$.

α (deg)	Φ_1	Φ_2
7.5	7.5×10^{-1}	9.25×10^{-1}
30.0	3.3486016×10^{-1}	6.2884169×10^{-1}
60.0	1.3410560×10^{-1}	3.1755495×10^{-1}
90.0	5.1104756×10^{-2}	1.2716367×10^{-1}
120.0	2.1465687×10^{-2}	2.2373903×10^{-2}
150.0	3.6396989×10^{-3}	1.6505689×10^{-4}

TABLE 1. Knots for splines used in Φ_1 and Φ_2.

The first derivatives (per radian) at the ends of splines are: $\Phi_1'(\frac{\pi}{24}) = -\frac{6}{\pi}$, $\Phi_1'(\frac{5\pi}{6}) = -9.1328612 \times 10^{-2}$, $\Phi_2'(\frac{\pi}{24}) = -\frac{9}{5\pi}$, $\Phi_2'(\frac{5\pi}{6}) = -8.6573138 \times 10^{-8}$, $\Phi_3'(0) = -0.10630097$, $\Phi_3'(\frac{\pi}{6}) = 0$.

α (deg)	Φ_3
0.0	1
0.3	8.3381185×10^{-1}
1.0	5.7735424×10^{-1}
2.0	4.2144772×10^{-1}
4.0	2.3174230×10^{-1}
8.0	1.0348178×10^{-1}
12.0	6.1733473×10^{-2}
20.0	1.6107006×10^{-2}
30.0	0

TABLE 2. Knots for spline used in Φ_3.

2.3. H,G_{12} **phase function.** G_1 and G_2 from the three-parameter phase function are replaced by a single slope parameter G_{12} which relates to the G slope parameter in the H,G system (though there is not an exact correspondence). The reduced flux densities can be obtained from [K. Muinonen et al. (2010)]:

$$10^{-0.4V(\alpha)} = L_0(G_1\Phi_1(\alpha) + G_2\Phi_2(\alpha) + (1 - G_1 - G_2)\Phi_3(\alpha)) \tag{9}$$

where:

$$G_1 = \begin{cases} 0.7527G_{12} + 0.06164, & \text{if } G_{12} < 0.2; \\ 0.9529G_{12} + 0.02162, & \text{otherwise;} \end{cases}$$
$$G_2 = \begin{cases} -0.9612G_{12} + 0.6270, & \text{if } G_{12} < 0.2; \\ -0.6125G_{12} + 0.5572, & \text{otherwise;} \end{cases} \tag{10}$$

$$H = -2.5 \log_{10} L_0; \tag{11}$$

and L_0 is the disk-integrated brightness at zero phase angle. The basis functions are as in the H,G_1,G_2 magnitude phase function. Coefficients L_0 and G_{12} are estimated from observations using non-linear least squares.

3. Numerical methods

3.1. **Least Squares.** Least-squares fitting is carried out in the flux-density domain, because it reduces the problem to a linear problem for the H,G_1,G_2 and H,G phase functions, and the errors are symmetric about the fit. The flux for the i^{th} observation is computed using:

$$\begin{aligned} L_i &= 10^{-0.4V_i}, \\ \sigma_i^{(L)} &= L_i(10^{0.4\sigma_i^{(V)}} - 1), \end{aligned} \tag{12}$$

where $\sigma_i^{(V)}$ are standard deviations of the magnitude measurements. The χ^2-value to be minimized here with respect to the parameters $\mathbf{a}$ is

$$\chi^2(\mathbf{a}) = \sum_{i=1}^{N} \frac{[L_i - L_i(\alpha_i, \mathbf{a})]^2}{[\sigma_i^{(L)}]^2}. \quad (13)$$

The computed disk-integrated brightnesses are expressed via N_a basis functions $\Phi_1(\alpha), \Phi_2(\alpha), \ldots, \Phi_{N_a}(\alpha)$:

$$L_i(\alpha_i, \mathbf{a}) = \sum_{l=1}^{N_a} a_l \Phi_l(\alpha_i). \quad (14)$$

For the H,G and H,G_1,G_2 phase functions, the $\mathbf{a}$ coefficients are fitted using linear least squares and for the H,G_{12} phase function the L_0, and G_{12} parameters are fitted using simplex non-linear regression [J. A. Nelder and R. Mead (1965)].

3.2. **Error estimation.** The absolute magnitude computation requires Monte-Carlo error estimation because of its nonlinearity. Gaussian errors in parameters a_1, and a_2 (in the H, G, phase function) or a_1, a_2, and a_3 (in the H,G_1,G_2 phase function) result in non-Gaussian errors in the H,G or H,G_1,G_2 parameters. To estimate those errors, we make use of the least-squares solution for a_1, and a_2 or a_1, a_2, and a_3 and its error covariance matrix. We set the error covariance matrix and the least-squares solution as a covariance and mean of a multi-normal distribution to produce a sample a_1, a_2 or a_1, a_2, a_3 using a multi-normal random number generator. The a_i samples are then converted to H,G or H,G_1,G_2 samples using either Eqs. 3 and 4 or 6, 7 and 8. Next, the samples are ordered in descending goodness of fit and then 68.27% (equivalent to 1-σ) and 99.73 % (equivalent to 3-σ) error cut-offs are computed, resulting in a list of subsamples. The limiting (maximum and minimum) H,G or H,G_1,G_2 parameters are selected from that list and the two-sided errors are computed.

Error estimation for the H,G_{12} parameters derives from the Markov chain Monte-Carlo (MCMC) technique. From non-linear least-squares fitting we obtain the least-squares values of L_0 and G_{12}. The errors in L_0, G_{12} are non-Gaussian, so the error estimation used for the H,G and H,G_1,G_2 phase functions cannot be used. To proceed, we create one long Markov chain by sampling possible L_0, G_{12} solutions. The chain is started at the least-squares point for L_0, G_{12}, and makes use of a multivariate Gaussian proposal distribution, where a covariance matrix for L_0, G_{12} is taken from the least-squares solution. After obtaining $10,000$ different solutions, the two-sided errors are computed based on the equivalents of the 1-σ and 3-σ cut-offs as in the H,G and H,G_1,G_2 phase functions. Error envelopes are based on the 1-σ and 3-σ Monte Carlo samples. We compute reduced magnitude for all the sampled values of H,G and/or H,G_1,G_2 and/or L_0, G_{12} for a set of phase angles, and choose the maximum and minimum of reduced magnitude at each phase angle.

3.3. **Fitting data for individual asteroids.** We start our computation by performing least-squares fits with all three phase functions, assuming 0.3 mag standard deviation for all of the observations (see section **??**). We extract magnitude residual rms value from that computation and repeat least-square fitting assuming magnitude uncertainties equal to the rms value for each phase function. Next, we perform the Monte-Carlo error computation to obtain two-sided errors in the photometric parameters, together with the error envelopes for the phase functions.

3.4. **Fitting data for asteroid families.** We fit family data sets using the H,G_1,G_2 phase function. Family membership was established by agglomerating asteroids in relative velocity phase space [M.-T. Enga et al. (2011, in prep.)]. Velocity cutoffs for each family are related to the background population velocity. We devise a 20×20(400 nodes) grid in G_1, G_2 phase space ($G_1 \in (0,1)$, $G_2 \in (0,1)$), and step through that grid. In each step, G_1, G_2 parameters are fixed to the node G_1, G_2 values, and for a number of asteroids in a given family ($i = 1, 2, ..., N$) a linear least-squares fit of L_{0_i} is performed. Global family χ^2 is computed assuming no correlation in the noise among different asteroids. From the 400 nodes we select the one with the best χ^2, and create a new, denser grid in the vicinity of that node (stretching 1-node distance on each side from the best χ^2 solution). We repeat the least squares analysis in the nodes of the new grid. This operation is repeated a number of times to obtain improved precision of the G_1, G_2 parameters. Once the family $G_{1,f}$, $G_{2,f}$ have been obtained, we perform Monte-Carlo error analysis in the $N + 2$ parameters phase space to obtain the two-sided 1-σ and 3-σ uncertainties.

4. Software description, requirements and dependences

The Asteroid Phase Function Analyzer is an online, free, interactive applet written in Java. It is cross platform and it runs in a Web browser using a Java Virtual Machine (JVM). It requirers 1.6 Java Runtime Environment (JRE).

The core of the applet constitutes a multi-threaded Java program composed of a number of packages, the contents of which are summarized in Table 3. The program uses the Java Scientific Library written by Flanagan []. The program is multi-threaded, and uses a thread pool pattern, in which a number of threads are created (one per computer core) to perform absolute-magnitude computations (one per asteroid) in parallel. Tasks are organized in a queue. As soon as the thread has completed a task, the next task from the queue is requested until all the tasks are completed. The programming details need not be known to applet users. The applet is straightforward and very easy to use. A user guide is also provided. It is, however, expected that the user be familiar with the methods behind state-of-the-art empirical phase-functions as well as non-Gaussian error estimation. The applet primarily produces absolute magnitudes and slope parameters, together with two-sided uncertainties for all three phase functions at the same time for a

Package	Classes included	Content
absoluteMagnitude	AsteroidData.java AsteroidPhotometricSolution.java AbsoluteMagnitude- CalculatorThreaded.java ThreadPool.java	Main package, with Thread Pool creating jobs (for different asteroids) and distributing them among cores. Contains data object and object with collected results.
phaseCurves	Function1D.java HGfunction.java HG1G2function.java HG12function.java	Contains the phase functions and methods for evaluating them for different sets of parameters.
regression	LinearRegressor.java FittedFunctionHG12.java FitterHG.java FitterHG1G2.java FitterHG12.java	Contains tools for performing linear and nonlinear least-squares phase-curve fitting and least-squares error analysis.
errorAnalysis	NonGaussianErrorEstimator.java MCMCSampler.java RandomNumberGenerator.java PdfComparator.java ParameterComparator.java PhaseCurveSolution.java	Contains methods for two-sided error estimation, a multinormal random number generator, a Markov-chain Monte- Carlo sampler, comparators.
inputOutput	DataFileReader.java OutputWriter.java Utils.java	Contains methods dealing with input/output.
ui	PhaseCurveAnalyserApplet.java DataEntry.java FileInputPane.java InputTableModel.java Task.java ResultPane.java Logger.java TextInputPane.java	Contains the applet and graphical user interface.

TABLE 3. Description of main packages

given data file. Other photometric parameters and plots are also produced. The tool is available at http://asteroid.astro.helsinki.fi/AstPhase/.

5. Testing the code

We compared the results obtained from this software and those from Fortran software [K. Muinonen et al. (2010)]. We have repeated calculations for all the asteroids listed in Table 4 using the same data and error estimates (that is, ± 0.03

mag uncertainty for all the objects except for the Moon, where we assume ± 0.023 mag uncertainty for phase angles $\alpha < 100^\circ$, and ± 0.2 mag uncertainty for phase angles $\alpha \geq 100^\circ$). Tables 5 and 6 contain the results obtained using Java software (I) and Fortran software (II). The results from [K. Muinonen et al. (2010)] and the Asteroid Phase Function Analyzer agree very well. There exist some small differences in the error analysis which can be explained by the limited number of samples in the Monte Carlo simulations.

Asteroid	Class	p_V	N_{obs}	α_{min}	α_{max}	References
(24) Themis	C, B	0.08	22	0.34	20.8	[Harris et al. (1989a)]
(44) Nysa	E	0.54	23	0.17	21.5	[Harris et al. (1989b)]
(69) Hesperia	M	0.14	21	0.13	16.0	[Poutanen et al. (1985)]
(82) Alkmene	S	0.21	11	2.29	27.2	[Harris et al. (1984b)]
(133) Cyrene	SR	0.26	11	0.20	13.2	[Harris et al. (1984a)]
(419) Aurelia	F	0.05	7	0.62	15.4	[Harris and Young (1988)]
(1862) Apollo	Q	0.26	18	0.2	89.0	[Harris et al. (1987)]
The Moon	-	0.17	17	0.5	140.0	[Bowell et al. (1989)]

TABLE 4. Objects used to illustrate the Asteroid Phase Function Analyzer capabilities. We show the V-band geometric albedo p_v [Tedesco, E.F. at al. (2002a)], the number of observations N_{obs}, the minimum and maximum phase angles of the observations α_{min} and α_{max}, and references to the observations.

6. Running instructions

6.1. **Processing single asteroid phase curve data.** Go to "File Input" tab, click "Load file", import data file from your file system (data file has to be in format specified below). Once the file is imported click Compute. Go to "Log" tab to trace the progress of computation. New tab with figures will appear. Go to that tab and switch between different phase function plots. To save the figures right click on the figure and pick "save as..." to save numerical results right click on the figure and pick "save numerical results as ...".

6.2. **Processing multiple asteroids at the same time.** Everything the same as for processing single asteroid phase curve, except that the data file contains many asteroids. File should be in the following format:

```
AsteroidDesignation NrOfDataPoints
PhaseAngle1 ReducedMagnitude1
PhaseAngle2 ReducedMagnitude2
PhaseAngle3 ReducedMagnitude3
.
```

Asteroid	H (II)	H (I)	G_1 (II)	G_1 (I)	G_2 (II)	G_2 (I)
(24) Themis	7.088	7.088	0.62	0.62	0.14	0.14
	-0.073	-0.069	-0.24	-0.25	-0.16	-0.16
	$+0.079$	$+0.084$	$+0.28$	$+0.26$	$+0.16$	$+0.15$
(44) Nysa	6.904	6.904	0.050	0.050	0.67	0.67
	-0.070	-0.068	-0.259	-0.275	-0.15	-0.17
	$+0.079$	$+0.079$	$+0.269$	$+0.299$	$+0.14$	$+0.14$
(69) Hesperia	6.927	6.927	0.36	0.36	0.29	0.29
	-0.069	-0.067	-0.25	-0.23	-0.18	-0.17
	$+0.069$	$+0.072$	$+0.28$	$+0.28$	$+0.16$	$+0.15$
(82) Alkmene	8.06	8.06	0.17	0.17	0.39	0.39
	-0.25	-0.25	-0.28	-0.27	-0.13	-0.12
	0.33	$+0.33$	$+0.46$	$+0.43$	$+0.11$	$+0.103$
(133) Cyrene	7.831	7.831	0.21	0.21	0.39	0.39
	-0.088	-0.088	-0.45	-0.43	-0.33	-0.39
	$+0.098$	$+0.098$	$+0.52$	$+0.52$	$+0.30$	$+0.32$
(419) Aurelia	8.49	8.49	0.95	0.95	-0.057	-0.057
	-0.14	-0.13	-0.54	-0.52	-0.399	-0.367
	$+0.16$	$+0.16$	$+0.69$	$+0.66$	$+0.318$	$+0.326$
(1862) Apollo	16.249	16.249	0.38	0.38	0.354	0.354
	-0.097	-0.097	-0.12	-0.12	-0.051	-0.051
	$+0.100$	$+0.105$	$+0.15$	$+0.15$	$+0.052$	$+0.053$
Moon	-0.126	-0.126	0.36	0.36	0.338	0.338
	-0.084	$-$ 0.085	-0.12	-0.12	-0.052	-0.048
	$+0.091$	$+0.090$	$+0.14$	$+0.14$	$+0.049$	$+0.049$

TABLE 5. Absolute magnitudes, and slope parameters with two-sided 99.73% errors. Comparison with Muinonen et al. [K. Muinonen et al. (2010)] for the H,G_1,G_2 phase function. (I) results obtained using the Java software, (II) results obtained using the Fortran software.

.
.
.

PhaseAngleN ReducedMagnitudeN

First line contains asteroid designation and N - number of data points to follow. Next N lines contain phase angles and corresponding reduced magnitudes. File can contain more then one object, the above record style would be then repeated and next asteroid record could be added following the first record. For example input files see "Example.txt" (below).

Asteroid	H (II)	H (I)	G_{12} (II)	G_{12} (I)
(24) Themis	7.121	7.121	0.68	0.68
	-0.042	-0.043	-0.23	-0.24
	$+0.044$	$+0.044$	$+0.25$	$+0.26$
(44) Nysa	6.896	6.896	-0.066	-0.066
	-0.041	-0.038	-0.077	-0.075
	$+0.044$	$+0.043$	$+0.072$	$+0.074$
(69) Hesperia	6.987	6.987	0.41	0.41
	-0.036	-0.041	-0.21	-0.22
	$+0.040$	$+0.043$	$+0.26$	$+0.28$
(82) Alkmene	8.187	8.187	0.30	0.30
	-0.032	-0.032	-0.14	-0.14
	$+0.034$	$+0.033$	$+0.19$	$+0.19$
(133) Cyrene	7.882	7.882	0.20	0.20
	-0.026	-0.027	-0.51	-0.016
	$+0.070$	$+0.03$	$+0.49$	$+0.015$
(419) Aurelia	8.514	8.514	1.04	1.04
	-0.074	-0.077	-0.46	-0.50
	$+0.052$	$+$ 0.084	$+0.16$	$+0.55$
(1862) Apollo	16.209	16.209	0.334	0.334
	-0.022	-0.024	-0.077	-0.081
	$+0.023$	$+0.025$	$+0.077$	$+0.078$
Moon	-0.124	-0.124	0.358	0.358
	-0.020	-0.020	-0.073	-0.075
	$+0.022$	$+0.021$	$+0.073$	$+0.074$

TABLE 6. Absolute magnitudes, and slope parameters with two-sided 99.73% errors. Comparison with Muinonen et al. [K. Muinonen et al. (2010)] for the H,G_{12} phase function. (I) results obtained using Java software, (II) results obtained using Fortran software.

7. Processing big amount of data

Download PhaseCurveAnalyzer.jar file and run it using:

```
java -jar PhaseCurveAnalyzer.jar Example.txt nrOfCores
```

ie.:

```
java -jar PhaseCurveAnalyzer.jar dataFile.dat 2
```

Output will be written to files on your disk. Output files will include:

- Plots:
  - *HGPhaseCurve.png

  - *HG1G2PhaseCurve.png
  - *HG12PhaseCurve.png
- Text files:
  - *.resultsSummary - summary of all the objects processed.
  - *.results - detailed output for each asteroid processed.

The files will be located in the input file directory.

8. Example input file

See the below example input file. Notice that asteroid name together with asteroid number is a single String!

"Example.txt"

```
(24)Themis 22
13.55 7.825
13.28 7.853
7.26 7.600
6.89 7.586
4.95 7.478
4.75 7.452
4.36 7.439
3.95 7.417
2.94 7.366
2.80 7.351
2.40 7.317
1.98 7.295
1.71 7.278
1.57 7.279
1.39 7.250
1.17 7.239
0.74 7.207
0.57 7.197
0.44 7.172
0.34 7.146
7.79 7.626
20.79 8.110
(44)Nysa 23
19.00 7.551
18.52 7.524
17.16 7.511
```

13.81 7.437
13.20 7.426
8.27 7.304
0.98 7.052
0.63 7.014
0.17 6.911
0.36 6.972
0.75 7.033
1.23 7.080
1.62 7.105
2.02 7.126
4.95 7.235
9.78 7.341
11.59 7.385
12.94 7.425
13.27 7.427
13.58 7.433
13.89 7.434
19.40 7.545
21.47 7.599
(69) Hesperia 21
16.00 7.82
12.19 7.71
11.90 7.68
11.62 7.67
9.89 7.64
5.10 7.48
4.04 7.42
3.26 7.28
2.46 7.25
1.67 7.13
1.28 7.12
0.92 7.08
0.13 7.00
0.29 6.99
1.04 7.10
2.23 7.23
5.69 7.43
6.03 7.43

8.59 7.53
12.72 7.64
13.00 7.69

9. Example results

For each asteroid three plots are produced: H, G phase function, H, G_1, G_2 phase function and H, G_{12} phase function. Example result plots are show in Fig. 1, 2, 3. File *.result which is a text file containing detailed numerical output is produced, and also a summary file *resultsSummary is produced.

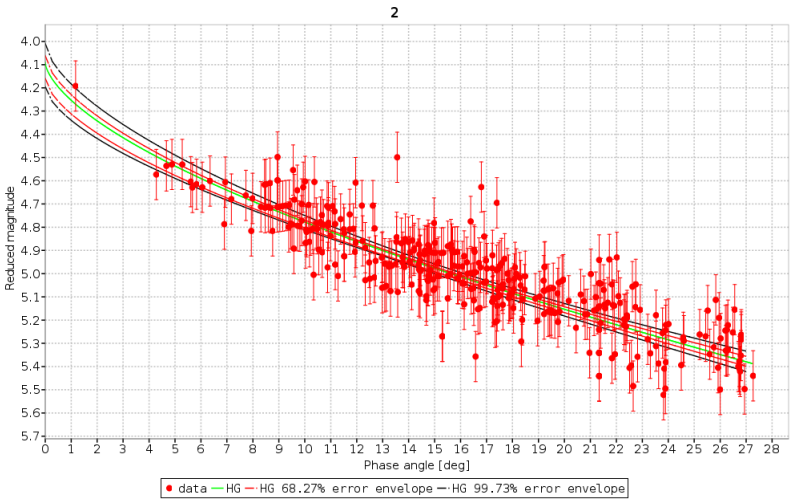

Figure 1. H, G phase function for asteroid (2) Pallas

10. Comments

Comments, bugs etc. can be reported to `dagmara.oszkiewicz@helsinki.fi`.

11. Acknowledgments

Research supported by the Magnus Ehrnrooth Foundation, Academy of Finland, Lowell Observatory, and the Spitzer Science Center. We would like to thank Michael Thomas Flanagan for developing and maintaining the Java Scientific Library, which we have used in the Asteroid Phase Function Analyzer. DO thanks Berry Holl for help with Java plotters and Saeid Zoonemat Kermani for valuable advice on Java applets. We thank the Department of Physics of Northern Arizona University for CPU time on its Javelina open cluster allocated for our computing.

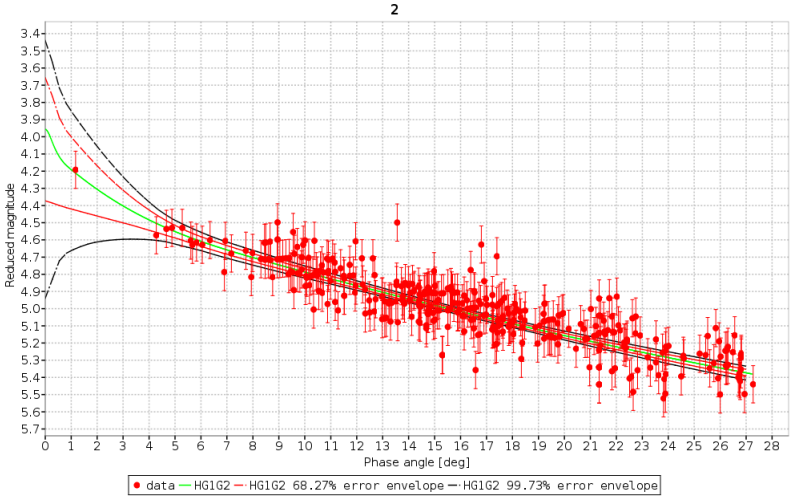

FIGURE 2. H, G_1, G_2 phase function for asteroid (2) Pallas

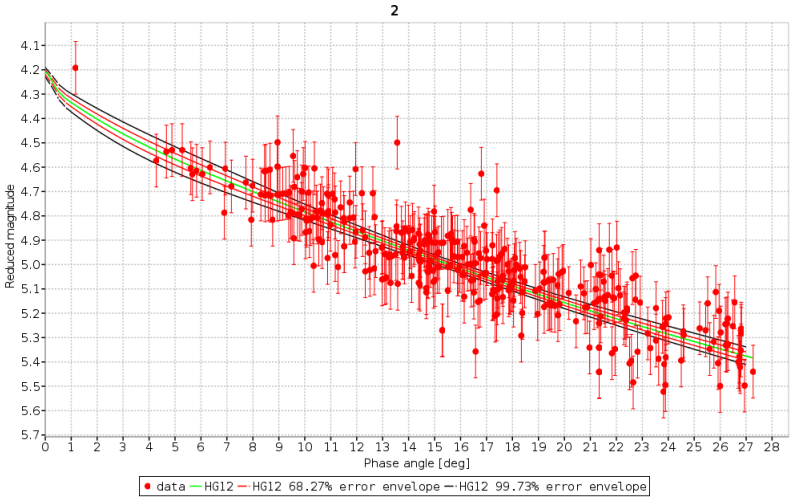

FIGURE 3. H, G_{12} phase function for asteroid (2) Pallas

REFERENCES

[Bowell et al. (1989)] Bowell E., Hapke B., Domingue D., Lumme K., Peltoniemi J., and Harris A. W. Application of photometric models to asteroids. In: T. Gehrels, M. T. Matthews, R. P. Binzel, editors. *Asteroids II*, University of Arizona Press; 1989, p. 524-555.

[K. Muinonen et al. (2010)] K. Muinonen, I. N. Belskaya, A. Cellino, M. Delbo, A.-C. Levasseur-Regourd, A. Penttilä, E. F. Tedesco. A three-parameter magnitude phase function for asteroids. *Icarus* 2010; 209: 542-555.

[J. A. Nelder and R. Mead (1965)] J. A. Nelder and R. Mead. A simplex method for function minimization *Computer Journal* 1965; 7: 308-313.

[Tedesco, E.F. at al. (2002a)] Tedesco, E.F., Noah, P.V., Noah, M., Price, S.D. *The supplemental IRAS minor planet survey. Astron. J.* 2002a; 123: 10561085.

[M.-T. Enga et al. (2011, in prep.)] M.-T. Enga et al. Asteroid family albedos from the Spritzer asteroid catalog *in preparation.*

http://www.ee.ucl.ac.uk/ mflanaga/java/ *Michael Thomas Flanagan's Java Scientific Library.*

ftp://ftp.lowell.edu/pub/elgb/astorb.html *The Asteroid Orbital Elements Database.*

[Zeljko Ivezic et al. (2001)] Z. Ivezic, S. Tabachnik, R. Rafikov, R. H. Lupton, T. Quinn, M. Hammergren, L. Eyer, J. Chu, J. C. Armstrong, X. Fan, K. Finlator, T. R. Geballe, J. E. Gunn, G. S. Hennessy, G. R. Knapp, S. K. Leggett, J. A. Munn, J. R. Pier, C. M. Rockosi, D. P. Schneider, M. A. Strauss, B. Yanny, J. Brinkmann, I. Csabai, R. B. Hindsley, S. Kent, D. Q. Lamb, B. Margon, T. A. McKay, J. A. Smith, P. Waddel and D. G. York Solar System objects observed in the Sloan Digita Sky Survey Commissioning data. *Astron. J.* 2001; 122:2749-2784

[C. T. Rogers et al. (2006)] C. T. Rodgers, R. Canterna, J. A. Smith, M. J. Pierce and D. L. Tucker Improved u'g'r'i'z' to UBVR$_C$I$_C$ transformation equations for main-sequence stars. *Astron. J.* 2006; 132:989-993.

[Harris et al. (1989a)] Harris A. W., Young J. W., Bowell E., Martin L. J., Millis R. L., Poutanen M., Scaltriti F., Zappalà V., Schober H. J., Debehogne H., and Zeigler K. W 1989a. Photoelectric observation of asteroids 3, 24, 60, 261, 863. *Icarus* 1989a; 77: 171-186.

[Harris et al. (1989b)] Harris A. W., Young J. W., Contreiras L., Dockweiler T., Belkora L., Salo H., Harris W. D., Bowell E., Poutanen M., Binzel R. P., Tholen D. J., and Wang S. Phase relations of high albedo asteroids: the unusual opposition brightening of 44 Nysa and 64 Angelina. *Icarus* 1989b; 81: 365-374.

[Harris et al. (1987)] Harris, A.W., Young, J.W., Goguen, J., Hammel, H.B., Hahn, G., Tedesco, E.F., Tholen, D.J. Photoelectric lightcurves of the Asteroid 1862 Apollo. *Icarus* 1987; 70: 246-256.

[Poutanen et al. (1985)] Poutanen M., Bowell E., Martin L. J., and Thompson D. T., Photoelectric photometry of asteroid 69 Hesperia. *Astron. Astroph. Suppl. Ser.* 1985; 61: 291-297.

[Harris et al. (1984b)] Harris A. W., Young J. W., Scaltriti F. and Zappalà V., The lightcurve and phase relation of the asteroids 82 Alkmene and 444 Gyptis. *Icarus* 1984b; 57: 251-258.

[Harris et al. (1984a)] Harris A. W., Carlsson M., Young J. W., and Lagerkvist C.-I., The lightcurve and phase relation of the asteroid 133 Cyrene. *Icarus* 1984a; 58: 246-256.

[Harris and Young (1988)] Harris, A. W., and Young J. W., Two dark asteroids with very small opposition effects. *Lunar Planet Sci.* 1988; XIX 2: 447-448

http://ssd.jpl.nasa.gov/sbdb.cgi *JPL Small-Body Database Browser.*

[NASA (2003)] NASA, Study to determine the feasibility of extending the search for near-Earth objects to smaller limiting diameters. *NASA Office of Space Science, Solar System Exploration Division, Washington DC.* 2003.